



## A self-charging cyanobacterial supercapacitor

Lin Liu, Seokheun Choi\*

Bioelectronics & Microsystems Laboratory, Department of Electrical & Computer Engineering, State University of New York-Binghamton, Binghamton, NY 13902, USA



### ARTICLE INFO

**Keywords:**

Photosynthetic microbial fuel cells  
Self-charging supercapacitors  
Supercapacitive energy harvesters  
Hybrid biodevices  
Double-functional bio-anodes

### ABSTRACT

Microliter-scale photosynthetic microbial fuel cells (micro-PMFC) can be the most suitable power source for unattended environmental sensors because the technique can continuously generate electricity from microbial photosynthesis and respiration through day-night cycles, offering a clean and renewable power source with self-sustaining potential. However, the promise of this technology has not been translated into practical applications because of its relatively low performance. By creating an innovative supercapacitive micro-PMFC device with maximized bacterial photoelectrochemical activities in a well-controlled, tightly enclosed micro-chamber, this work established innovative strategies to revolutionize micro-PMFC performance to attain stable high power and current density ( $38 \mu\text{W}/\text{cm}^2$  and  $120 \mu\text{A}/\text{cm}^2$ ) that then potentially provides a practical and sustainable power supply for the environmental sensing applications. The proposed technique is based on a 3-D double-functional bio-anode concurrently exhibiting bio-electrocatalytic energy harvesting and charge storing. It offers the high-energy harvesting functionality of micro-PMFCs with the high-power operation of an internal supercapacitor for charging and discharging. The performance of the supercapacitive micro-PMFC improved significantly through miniaturizing innovative device architectures and connecting multiple miniature devices in series.

### 1. Introduction

There is an intensive effort to enable a next-generation of smart, stand-alone, always-on wireless sensors networks (WSNs) designed to collect real-time information for human safety and security (Hu et al., 2011; Wu et al., 2017; Wang and Wu, 2012; Zanella et al., 2014; Dewan et al., 2014). The key challenges for these systems include improving the power efficiency of sensors to extend their lifetimes, and improving energy harvesting capability to provide them with sustainable power by converting ambient energy into electrical energy. An indication of how serious the former challenge is regarded is the Near Zero Power RF and Sensor operations (N-ZERO) program established by the Defense Advanced Research Projects Agency (DARPA). That program seeks to overcome the power limitations of persistent sensing remaining with even state-of-the-art battery technologies (Qian et al., 2017; Rajaram et al., 2018). Meanwhile, various energy harvesting techniques at the micro- or even nano-scale have been studied extensively for stand-alone WSN operation during the past decade (Wang and Wu, 2012; Cook-Chennault et al., 2008). Power can be scavenged from ambient thermal, kinetic, or solar energy; the choice of energy type is highly dependent upon the application (Selvan and Ali, 2016; Soavi et al., 2016). Among possible technologies, microliter-scale photosynthetic microbial fuel cells (micro-PMFCs) can offer the most suitable power source for

remote sensing in natural environments because subcellular or cellular photosynthetic components (e.g. oxygenic photosynthetic reaction centers, thylakoid membranes, cyanobacteria, or algae) can harvest the most abundant energy source, solar energy, to produce electrical power even in extreme conditions (Singh and Gabani, 2011; Choi, 2015; Bombelli et al., 2015; McCormick et al., 2015). PMFCs are a type of bioelectrochemical system in which living photosynthetic organisms (cellular) or non-living photosynthetic proteins (sub-cellular) harvest electrical power from solar energy (Choi, 2015; Bombelli et al., 2015; McCormick et al., 2015; Malik et al., 2009; Lea-Smith et al., 1857). Typically, PMFCs with living whole cells are far more resilient and significantly more robust than systems using sub-cellular photosynthetic proteins, and they provide superior self-repairing and self-assembling features (McCormick et al., 2011, 2015; Sekar and Ramasamy, 2015; Bombelli et al., 2011, 2012). Furthermore, cellular PMFCs can generate electricity continuously from microbial photosynthetic and respiratory activities under day-night cycles in the absence of an organic feedstock (McCormick et al., 2011; Bombelli et al., 2011, 2012). Despite the vast potential and promise of cellular PMFCs, their performance remains insufficient to realize potential WSN applications. To date, no micro-PMFCs exist that can independently power real-world sensor applications. These gaps have relegated today's PMFCs to the status of a laboratory curiosity rather than being a viable

\* Corresponding author.

E-mail address: [sechoi@binghamton.edu](mailto:sechoi@binghamton.edu) (S. Choi).

alternative power source. Their power densities, which are typically a couple of orders of magnitude lower than even the smallest power biological fuel cells, remain a significant challenge. Even the latest micro-PMFC system was limited to low power density ( $\sim 10 \mu\text{W}/\text{cm}^2$ ) and short operation time ( $\sim 2 \text{ h}$ ) (Bombelli et al., 2015). If one of the biggest arguments for micro-PMFC technology is its potential as a superior substitute to conventional batteries and other energy harvesting devices for future WSN applications, then there is a clear and pressing need to discover powerful yet simple approaches to enabling high-performance, self-sustaining, long-life micro-PMFCs, and to ensuring their practical feasibility as a power source for WSNs.

The key advantage of cellular micro-PMFCs over other types of small-scale energy sources is that their construction, fuel sources, and operation are environmentally friendly and entirely self-sustainable. Their cost of manufacture is low and their electricity production has the potential to be continuous for months or years, so long as there are periodic day-night cycles. Their primary disadvantage, however, is low energy production, which limits the technology to low power applications. Capacitors have been externally connected to the bioelectrochemical systems to boost the low power (Ren et al., 2013; Hatzell et al., 2013). The external capacitors are recharged by bioelectrochemical systems and produce high electrical output during the discharge. This connection technique has been demonstrated by several groups powering actual electronic devices. However, these external capacitors increase the cost of the system and require substantial recharging time – on the order of hours or even days – at the low current regimes of bioelectrochemical systems.

Recently, there is an innovative trend to develop an entirely new kind of electric power device: a self-charging supercapacitor (or a supercapacitive energy harvester) in which electric energy is simultaneously acquired and stored within a miniaturized single unit (Chen, 2017; Dubal et al., 2015; Pankratov et al., 2014a). This new hybrid device integrates the high-energy harvesting function of an energy generating device (e.g. fuel cells) with the high-power operation of an internal supercapacitor for charging and discharging. In particular, several proposals and preliminary demonstrations of the hybrid devices combine supercapacitors and bioelectrochemical systems such as enzymatic fuel cells, and heterotrophic MFCs (Villarrubia et al., 2016; Xiao et al., 2017; Houghton et al., 2016; Pankratov et al., 2014b; Alsaoub et al., 2017). This concept indicates the possibility that even low-performance micro-PMFCs can become a superior substitute for conventional batteries or other energy harvesting techniques.

A couple of sub-cellular PMFCs using thylakoid membranes have been combined with internal supercapacitors for simultaneous solar energy conversion and storage (Gonzalez-Arribas et al., 2017; Pankratova et al., 2017). Their power performance was five times greater than the value for the supercapacitive enzymatic fuel cells, demonstrating a clear proof-of-principle of this solar-driven self-charging biosupercapacitor (or a supercapacitive PMFC). However, the practical applications for sub-cellular systems are limited by the low stability of the sub-cellular components, leading to very short operating times. The sub-cellular PMFCs provided power for a maximum of only 30–40 min followed by a rapid loss of their electron transfer activity. Furthermore, they are subject to interruption, including significantly reduced energy production at night and on cloudy days because they cannot perform respiratory function. A self-charging biosupercapacitor (or a supercapacitive PMFC) with whole photosynthetic organisms using intact cyanobacterial cells could become a permanent power source for supplying long-term and stable power for small, wireless sensors used at remote sites where frequent battery replacement is impractical.

## 2. Results and discussion

By periodically connecting and disconnecting the bioelectrochemical systems to an external load, several studies demonstrated

that some type of exoelectrogens (e.g. *Geobacter sulfurreducens*, *Shewanella oneidensis* MR-1, and other mixed cultures) can store an excess of electrons under electron acceptor limitation (Malvankar et al., 2012; Uria et al., 2011; Ren et al., 2015). By closing the circuit, the stored electrons are discharged in intermittent current pulses that are stronger than under the steady-state power generated from continuous operation. These exoelectrogens exhibit pseudocapacitive behavior from the redox-active nature of biofilm (i.e. faradic electron transfers). Other research groups provided double-layer capacitance to the bioelectrochemical systems by inserting a capacitive layer between exoelectrogens and anode (Deeke et al., 2012, 2013, 2015). This capacitive layer generated more electricity compared with a non-capacitive electrode. The greater performance observed in these studies provided motivation and key components of a foundation for a supercapacitive micro-PMFC as a potentially viable long-term, self-sustaining, and high-performance method for energy generation and storage.

### 2.1. Device concept and design

In this work, we for the first time demonstrated a supercapacitive micro-PMFC featuring self-sustainable bacterial photoelectrochemical activities with supercapacitive performance in a well-controlled, tightly enclosed micro-chamber (Fig. 1a). The anode was based on a 3-D double-functional electrode concurrently exhibiting solar-driven energy-generating and storing features so that it offers the high-energy harvesting function of PMFCs and the high-power operation of an internal pseudocapacitor (Fig. 1b). The novel anodic structure was constructed by a 3-D conformal modification of carbon cloth fibers with the conductive polymer poly(3,4-ethylene dioxythiophene):polystyrene sulfonate (PEDOT:PSS) (Fig. 1c) (Liu and Choi, 2017; Pang et al., 2018a, 2018b). Previously, PEDOT:PSS was conformally coated over fibers of papers, carbon clothes, and various fabrics and its properties for biofilm formation were well characterized (Liu and Choi, 2017; Pang et al., 2018a, 2018b). The 3-D microporous carbon cloth with a large, accessible surface area can enable sufficient substrate/products exchange to support colonization of bacterial cells deep inside the anode (Liu and Choi, 2017). The addition of conductive polymers to the carbon cloth can improve the overall capacitance of cyanobacterial bioanode, where pseudocapacitance arises from irreversible charge transfer within the biofilm (Pankratov et al., 2014c) and reversible redox reactions at the PEDOT:PSS surfaces (Fig. 1d) (Park et al., 2013; Volkov et al., 2017; Kim et al., 2017). This is very interesting because photocatalytic reactions of cyanobacterial biofilm self-sustainably produced dense concentrations of electrons and protons for supercapacitive energy storage even in LB media that was ion-depleted after several days of operation. Evidently, the capacitance was negligible without biofilm formation on the anode, which indicates that the redox process from the PEDOT:PSS on the carbon cloth did not generate supercapacitive behavior in the ion-limited environment (Fig. 1d). In the cyanobacterial biofilm, electrons are recovered through a water-splitting reaction and/or photosynthetic electron transport chain during light illumination, followed by the respiratory activities (McCormick et al., 2015; Lea-Smith et al., 1857; Sekar and Ramasamy, 2015). With the conductive polymers, charge transfer reactions across the biofilm-polymer interface are performed through oxidation and reduction of PEDOT:PSS (Park et al., 2013; Volkov et al., 2017; Kim et al., 2017). Both redox interactions in the biofilm and polymer generate pseudocapacitance. The pseudocapacitive biofilm and polymer were formed on the double-layer capacitive carbon clothes, and the double-layer capacitance was aroused from the charge separation at the cathode. That means it's likely the pseudocapacitive and double-layer capacitive components were superimposed on each other and showed ambiguous redox peaks on top of a quasi-rectangular cyclic voltammetric response (Fig. 1d) (Pankratov et al., 2014c). Open circuit voltage ( $V_{oc}$ ) was determined by the equilibrium potentials of the electrodes (Fig. 1b). The photo-bio-electrocatalytic and redox reactions (i.e. a faradaic process or

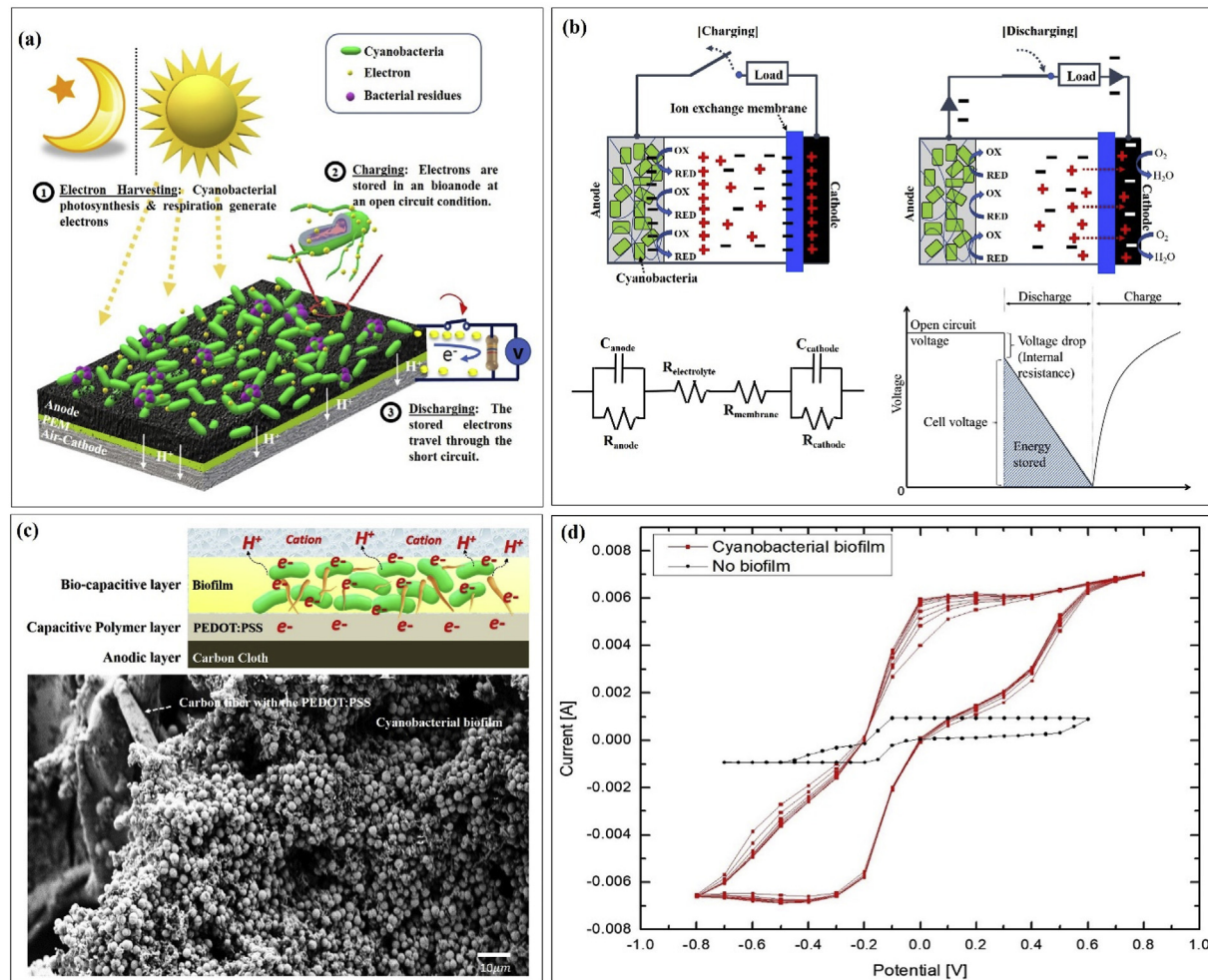


**Fig. 1.** (a) Conceptual diagram of the self-charging cyanobacterial supercapacitor. (b) Schematic diagram of the device during charging (left) and discharging (right) and its equivalent circuit with a representative voltage profile. (c) Schematic illustration of the 3-D double-functional bioanode and its SEM image. (d) Cyclic voltammetry of the anode with or without biofilm at a scan rate of 50 mV/s (PEM: proton exchange membrane).

pseudocapacitance) polarize the anode and cathode toward values that are more negative and positive than the typical equilibrium potential. Excess negative and positive charges at the electrodes are balanced by counter ions from the electrolyte forming an electrochemical double layer at each electrode of the device. However, it should be noted that the anode modification with biofilm and PEDOT:PSS likely decreased the double-layer capacitance even though the bioanode possessed pseudocapacitance and double-layer capacitance (Pankratov et al., 2014c).

After the hybrid device electrostatically stored charges, the device was discharged by a rapid electrostatic process under the short circuit condition; the energy electrostatically stored can be delivered with strong and short discharge pulses and high-power output can be achieved. During the discharge mode, the voltage dropped to a lower value because of the equivalent series internal resistances of the device;  $R_{anode}$ ,  $R_{electrolyte}$ ,  $R_{membrane}$ , and  $R_{cathode}$  are anodic, electrolyte, membrane, and cathodic resistance, respectively (Fig. 1b). Therefore, the output voltage of the device ( $V_{output}$ ) is related to  $V_{oc}$  and the internal resistances by Equation (1):

$$V_{output} = V_{oc} - I_{discharge}(R_{anode} + R_{electrolyte} + R_{membrane} + R_{cathode}) \quad (1)$$

where  $I_{discharge}$  is defined as the discharged current generated from the stored energy. This peak current decreases gradually to a base value that is a pure current production by cyanobacterial photosynthesis and respiration. While conventional supercapacitors offer a very fast

sequence of reversible charge separation and/or redox reactions, our supercapacitive PMFC can be relatively slow because of the irreversible charge transfers and the protons' long traveling distance. During the discharging operation, the electrons flow through the external circuit to reach the cathode while the protons diffuse from the anode to the cathode through the ion exchange membrane to maintain charge neutrality. Then, an electron acceptor, oxygen, is reduced by the protons and electrons that traveled from the anode. In particular, large  $R_{electrolyte}$  and  $R_{membrane}$  can originate from a poor transfer of protons, leading to a limiting energy bottleneck in the supercapacitive PMFCs. To effectively minimize those internal resistances, we reduced the proton traveling distance by designing a sandwiched electrode configuration where the ion exchange membrane (i.e. Nafion 117 membrane) was directly between the anode and the air-cathode.

The total device capacitance ( $C_{device}$ ) can be calculated using the following equation, which includes  $C_{anode}$  and  $C_{cathode}$ :

$$C_{device} = \frac{1}{V_{oc}} \int I_{discharge} dt = \left( \frac{1}{C_{anode}} + \frac{1}{C_{cathode}} \right)^{-1} \quad (2)$$

The supercapacitive micro-PMFC consisted of six functional layers; a bottom PMMA layer including a sandwiched PMFC in the middle, the 1st rubber gasket layer, the 2nd rubber gasket layer, a PMMA reservoir layer, a polydimethylsiloxane (PDMS) gas permeable layer, and a top polymethyl methacrylate (PMMA) layer (Fig. 2a). All layers were well aligned and assembled with screws. The rubber layers enabled a well-packaged, tightly-enclosed microchamber while the PDMS gas layer

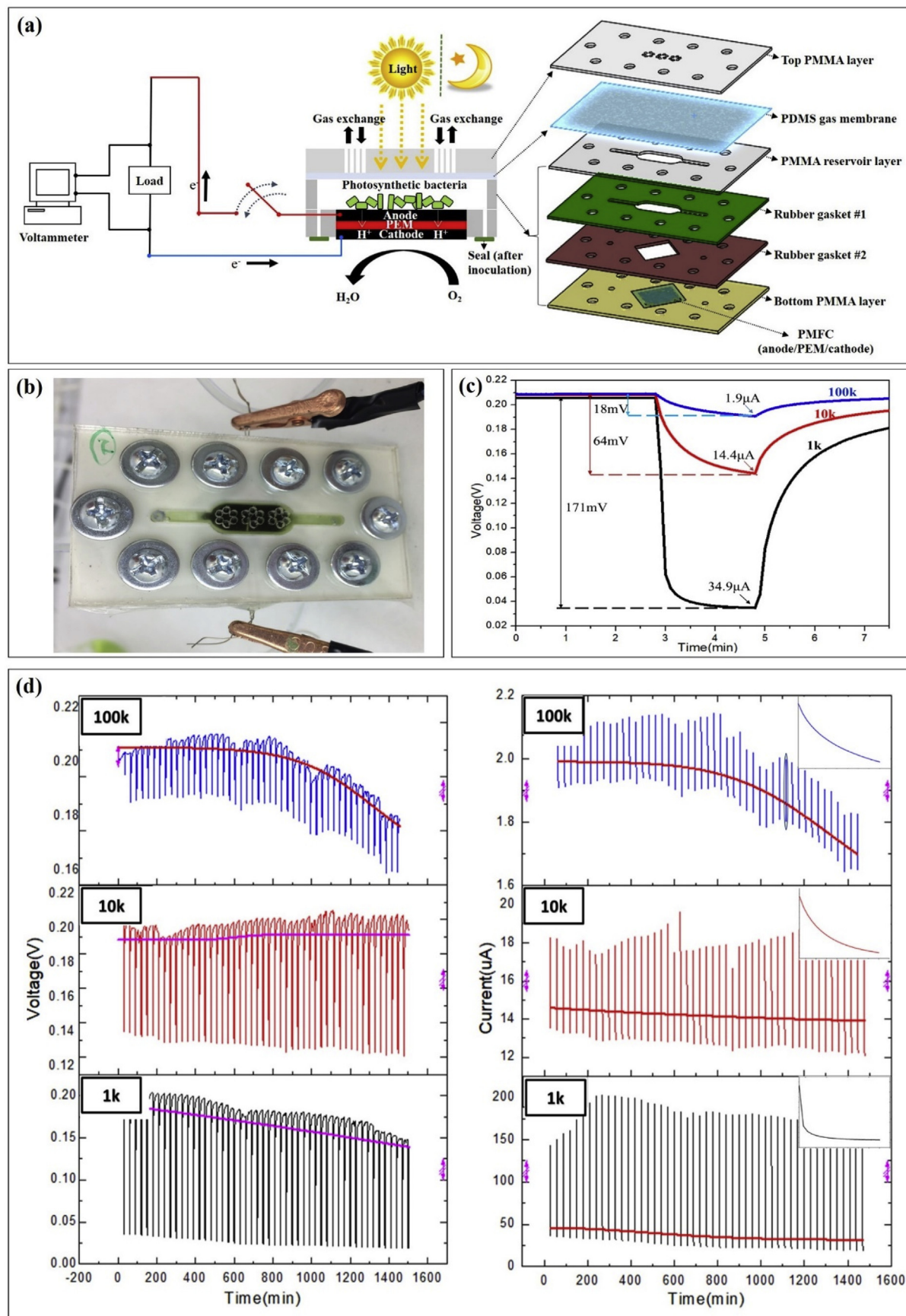


**Fig. 2.** (a) Schematic illustration of individual layers of the self-charging micro-PMFC, (b) photo of the assembled device, (c) discharging characteristic with different external resistors ( $1\text{k}\Omega$ ,  $10\text{k}\Omega$  and  $100\text{k}\Omega$ ), and (d) charging-discharging voltage and current curves with different external resistors. (Insert: magnification of a charge/discharge current cycle).

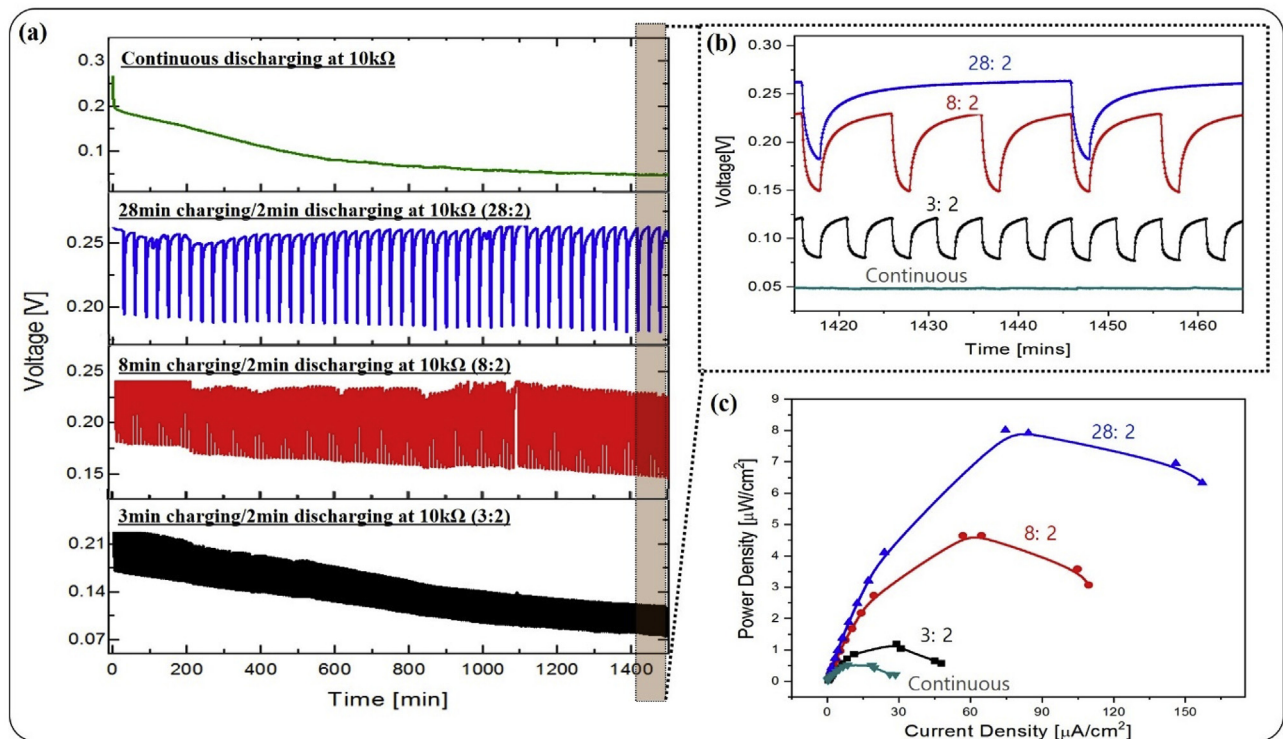


**Fig. 3.** (a) Output voltage profiles during different charging/discharging conditions at 10 kΩ, (b) magnification of their final charging/discharging cycles. (c) their power outputs as a function of current densities.

allowed necessary gases to reach the chamber for self-sustaining bacterial photosynthesis and respiration. The device configuration was based on our recently reported PMFC (Liu and Choi, 2017). The photosynthetic bacterial cells, *Synechocystis* sp. PCC 6803, introduced to the microchamber, were accumulated on the modified anode, forming a biofilm during 3 days (Fig. 2b). Their power and current densities were monitored under the operational condition of continuous light illumination at 30 °C. PEDOT:PSS coated on the carbon cloth improved conductivity, biocompatibility and surface affinity for the microorganisms (Marzocchi et al., 2015; Liu et al., 2015). This polymer treatment did not change the carbon fiber's thickness or pores and the deposition was very conformal and tight (Fig. S1). The 3-D microporous anodic structure allowed the photosynthetic bacterial cells to enter deep inside the anode and form a densely packed biofilm (Fig. 1c), ultimately leading to higher and longer performance of the micro-PMFC (Liu and Choi, 2017).

## 2.2. Effects of external resistance on device performance

Because the power generated from bacterial photosynthesis and respiration in the micro-PMFC is subject to the process of charging and discharging through periodic interruptions of the external circuit, it is critical to evaluate the effect of the external resistance on device performance, including discharging characteristics, capacitance, and durability.

Fig. 2c shows discharging characteristics of the device (supercapacitor??) when connected for 2 min to external loads of 1 kΩ, 10 kΩ, and 100 kΩ. Before each connection, the device had been charged for 28 min. At 1 kΩ, the voltage rapidly dropped within 1 min and stabilized at 37 mV, corresponding 34.9 μA. At 10 kΩ and 100 kΩ, the device required the prolonged discharge time where the voltages (143 mV and 193 mV, respectively) are more positive than under the 1 kΩ operation with 2 min of discharging time. The total capacitance discharged for 2 min was calculated by Equation (2), which were 0.63 mF, 5.2 mF, and 74.9 mF at 100 kΩ, 10 kΩ, and 1 kΩ, respectively (corresponding to

1.64 mF/cm², 13.51 mF/cm², 194.55 mF/cm², respectively). The external resistance clearly regulates the discharge rate of the accumulated energy during the discharging operation. A lower external resistance allows a more rapid discharge of the stored charges, thus producing higher current and capacitance while the device with a higher external resistance holds some of the stored energy after allowing a small current. Furthermore, the operational stability of the device was evaluated by repeating charge-discharge cycles (Fig. 2d). An automated charging-discharging operation was performed using an Arduino connected to relays to enable accurate period switching (Fig. S2). Fig. 2d shows the voltage and current profiles of the supercapacitive micro-PMFC at different external resistances with 28 min charging and 2 min discharging. Each cycle repeated indicating the reversibility of the process. While the single discharging profile demonstrated that the low external resistance at 1 kΩ provides the better capacitive and electrical performance (Fig. 2c), the durability of the established voltage and thus the stability of the device at 1 kΩ degraded over time (Fig. 2d). This is mainly because the mass transport rate from the substrates is slow at high current and shortens current production. The low external resistance rapidly released the stored charges, requiring more charges to flow from bacterial metabolism. On the other hand, a high external resistance at 100 kΩ worsened the device stability than did the 1 kΩ resistance. The high external resistance discharged small current because of the reduced flow of electrons through the circuit, leaving the majority of the charge in the bacterial membrane and the anode. This retarded electron transfer decreased bacterial growth, metabolism and thus the stability of the device (Uria et al., 2011; Picioareanu et al., 2008; Katuri et al., 2011). Although the device was not fully discharged at 10 kΩ (Fig. 2c), the output voltage and current remain stable through a period of 24 h (Fig. 2d). This demonstrates that the durability and stability of the device at 10 kΩ was the best, which could be matched to an external load as a self-sustained power supply. These results indicate that the selection of external resistance is important in device performance.

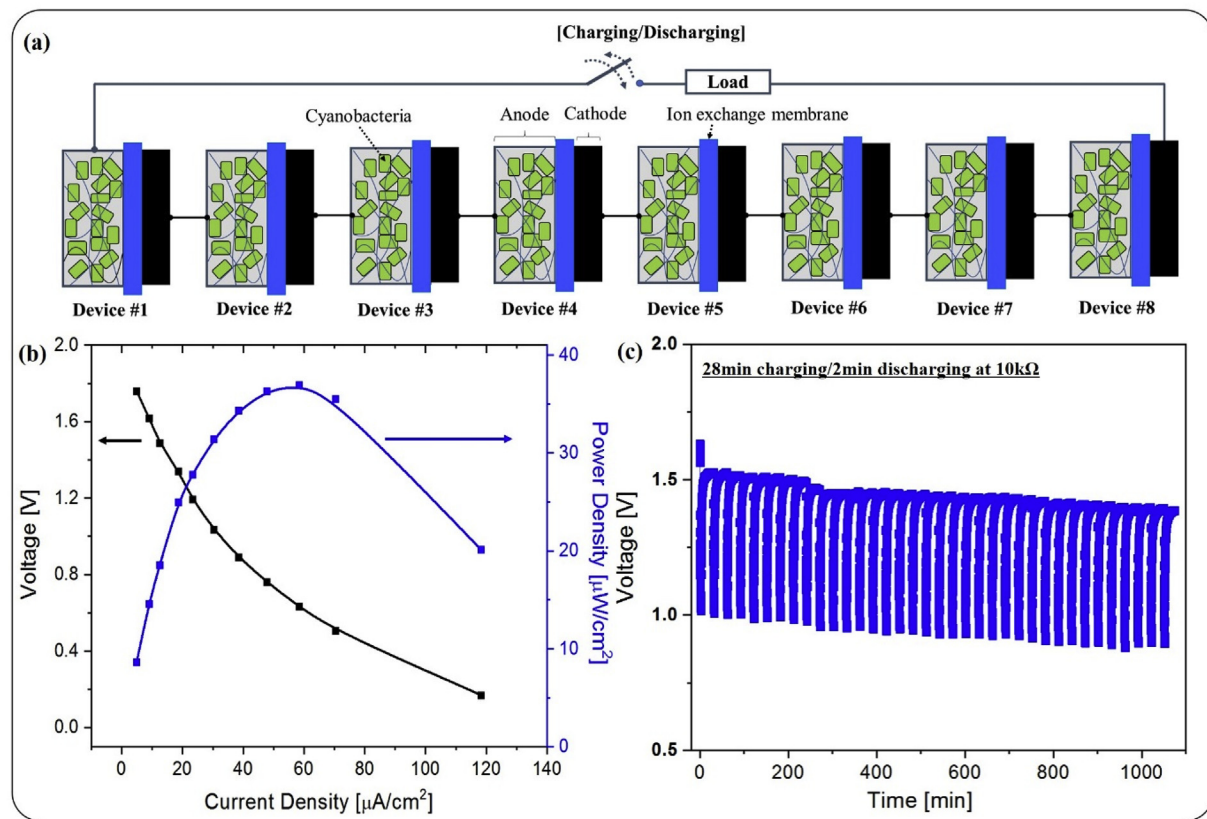


**Fig. 4.** (a) Schematic diagram of the stacked device connecting eight units in series, (b) polarization curve and power output of the stacked device, and (c) its charging/discharging cycles.

### 2.3. Charging time and durability

The charging is substantially slower than the discharging because the process is not reversible in our supercapacitive PMFC and the charging requires time for harvesting electrons and protons via bacterial photosynthesis and respiration. Therefore, optimizing the charging time with the respect to a certain discharging condition is very important as the amount of the stored charges determines the device open circuit voltages (OCVs), output voltages at a discharging mode, power and current generations, and durability of the established voltages. 3 min, 8 min, and 28 min charging times were tested and their performances were compared with the continuous discharging operation (Fig. 3). For all these experiments, the discharging time and the external resistance were fixed with 2 min and 10 k $\Omega$ , respectively, which maximized the device performance in the previous section. Under the continuous discharging mode without charging process, the device acted as a PMFC only without the supercapacitive operation (Fig. 3a). The output voltage of the continuous discharging operation significantly decreased for the first 600 min and then gradually decreased to 0.05V (corresponding to 5  $\mu\text{A}$ ) during the next 800 min. This is because the number of electrons harvested from bacterial metabolism was not enough to allow the current flow through the 10 k $\Omega$  resistor. With the device operating discontinuously, charges were accumulated on the bioanode on the open circuit. During the short circuit, the stored charges were burst, generating greater output voltages at charging/discharging modes, power and current densities, and durability than the continuous discharging operation. Three minutes of charging allowed more charges to be stored, increasing the output voltage by 40% and the maximum power/current by 100%, compared to the continuous operation (Fig. 3b). However, the durability of the voltages degraded over time, indicating that the 3 min charging time was not enough to restore the equilibrium electrode potentials and recharge the device at

the OCV. Overcoming the resistance at 10 k $\Omega$  so the current would discharge the device required more charges than were stored during a 3-min charging time. The durability significantly improved by increasing the charging time to 8 min. However, a slight degradation of durability was shown during 24 h which indicates that the device has the capacity to store more charges for the 2 min discharging operation at 10 k $\Omega$ . During the 8 min test, the device's power generation outperformed the continuous discharging operation by a factor of 9 and the 3 min charge and 2 min discharge configuration by a factor of 4.5 (Fig. 3c). With 28 min of charging, the output voltages for the charging/discharging modes, the maximum power and current densities, durability and stability of the device were significantly improved. The maximum power and current densities were 8  $\mu\text{W}/\text{cm}^2$  and 160  $\mu\text{A}/\text{cm}^2$ , which are 16-fold and 5-fold larger than with the continuous discharging device (Fig. 3c). The durability and stability for the 28 min charging/2 min discharging case were also proven over 50 charging/discharging cycles without any performance decrease (the second figure of Fig. 1a). However, the further enhanced charging time decreased the device performance (data not shown) mainly because the longer charging time inhibited bacterial metabolism and even their viability, limiting a stable, long-time operation.

### 2.4. Stacking of supercapacitive PMFCs

Stacking the supercapacitive PMFCs in series is critical to increasing output voltage and power for practical applications. However, connecting multiple biological devices may be much more complicated than connecting conventional batteries or supercapacitors because live cyanobacterial behavior is unpredictable and irreproducible, leading to a significant performance degradation because of a different impedance mismatch between stacked devices. Unequal performance of individual devices can reverse voltage polarity in lowest performing device in the

stacked system, which lowers the voltage the whole system can produce (Wei et al., 2016). In this work, eight supercapacitive PMFCs were successfully connected in series, and each worked at full capacity (Fig. 4a). The novel microfabricated device offered precise control of the bioanode for optimal biofilm formation, minimizing the performance variation of individual devices. The OCV of the stacked array was 1.8V, which is equal to the sum of each device's OCV, about 0.225V (Fig. 4b). The maximum power and current density were  $38 \mu\text{W}/\text{cm}^2$  and  $120 \mu\text{A}/\text{cm}^2$ , respectively, which is the highest reported success of any existing micro-PMFCs for the long-term operation. The energy density for two 28 min charging/2min discharging operations per hour was  $2.52 \mu\text{Wh}/\text{cm}^2$ . With 28 min charging and 2 min discharging operation at  $10 \text{k}\Omega$ , the cycling stability was maintained through 18 h (Fig. 4c). A slight degradation was mainly because of small performance mismatch between devices which were located at different distances from the light source, leading to different photocatalytic reactions. Further studies will be required to optimize device stacking.

### 3. Conclusion

We created innovative supercapacitive micro-PMFCs with maximized bacterial photoelectrochemical activities in a well-controlled, tightly enclosed micro-chamber. An internal supercapacitor was integrated into a micro-PMFC device, where charge-storage and energy harvesting function simultaneously. During the charging-discharging operation with 28 min of charging and 2 min of discharging at  $10 \text{k}\Omega$ , our device produced a maximum power density of  $8 \mu\text{W}/\text{cm}^2$  and current density  $160 \mu\text{A}/\text{cm}^2$ , a performance significantly greater than that of the continuous discharging mode. The array of eight devices connected in series increased the output voltage (1.8 V) and power density ( $38 \mu\text{W}/\text{cm}^2$ ) significantly without showing any performance degradation. Further device improvement for practical applications can be made by using new materials with a high supercapacitive performance. Because solar energy is the most promising source of sustainable energy even in resource-limited environments, and photosynthetic organisms occupy every habitat, including those with extreme conditions, the supercapacitive micro-PMFCs can be an important and novel technology breakthrough that offers a potentially viable long-term and high-performance resource for unattended environmental sensors.

### 4. Experimental sections

**Materials:** Polydimethylsiloxane (PDMS) and its curing agent (Sylgard 184 Silicone Elastomer kit) were purchased from Dow Corning. 30% wet-proofed carbon cloth (CCWP), untreated carbon cloth (CCP10), carbon black powder (XC-72), and 10% Pt on Vulcan XC-72 were obtained from Fuel Cell Earth LLC. Dimethyl sulfoxide (DMSO), polytetrafluoroethylene (PTFE), Nafion solution, Nafion 117 membrane, glutaraldehyde, phosphate buffer saline (PBS), and poly (3,4-ethylenedioxothiophene):polystyrene sulfonate (PEDOT:PSS) were purchased from Sigma-Aldrich.

**Electrode preparation:** The anode was prepared on the untreated carbon cloth by brush-painting a mixture of 1 wt% PEDOT:PSS. 5 wt% DMSO was added to increase the anodic conductivity. The air-cathode was prepared on 30% wet-proofed carbon cloth with four layers of a mixture of carbon powder and PTFE solution (Cheng et al., 2006). The other side of the cathode was coated by 10% Pt on carbon black and a binder solution including 5 wt% Nafion solution, DI water, and isopropanol. The anodes and cathode were pierced with a 0.5 mm thick Ti wire as a current collector.

**Gas membrane preparation:** A PDMS solution (Sylgard 184 Silicone Elastomer kit) was prepared by mixing the pre-polymer and the curing agent in 10:1 ratio by weight. The PDMS mixture was degassed in a vacuum desiccator for about 30 min and then a 40  $\mu\text{m}$ -thick PDMS membrane was obtained on a glass wafer (Pyrex) with the high 1500 rpm spin speed for 30 s followed by curing in oven of 100 °C for

1 h. The solidified PDMS membrane was cut from the wafer, gently peeled off, and then transferred between the top and the reservoir layers (Liu and Choi, 2017).

**Device fabrication:** The Nafion 117 membrane was hot-pressed directly between the anode and the cathode to form a PMFC. A top PMMA layer, a PDMS gas permeable layer, a PMMA reservoir layer, two rubber gasket layers, and a bottom PMMA layer including the PMFC in the middle (Fig. 2a). The PMMA and rubber layers were cut by a laser machine (Universal Laser System, VLS3.5). All layers were carefully aligned and assembled with 10 small screws. The anodic surface area exposed to bacteria was  $0.385 \text{ cm}^2$  while the cathodic surface was  $0.636 \text{ cm}^2$ . Fluidic inlet and outlet tubes were connected to the device, but the tubes were removed after bacterial inoculation. For sustainable operation, the holes for the tubes were completely sealed with silicone. The volume of the PMFC chamber was  $90 \mu\text{L}$ .

**Electrical measurements:** Electrical potentials between the anodes and cathodes were monitored by a data acquisition system (DI-720-EN, DATAQ Instruments). The polarization and power curves were measured with a custom-made interface circuit, which measures the maximum current value at various external resistances. All the output values were measured after the device was fully charged. The current through a resistor was calculated using Ohm's law. Current/power density and areal capacitance were normalized to the anode area ( $0.385 \text{ cm}^2$ ). The energy density  $E (\mu\text{Wh}/\text{cm}^2)$  was calculated from the total power density over the discharge time ( $E = (P \times \text{discharging time})/3600$ ). All the experiments were done in the temperature/light-controllable incubator (The VWR® Signature™ Diurnal Growth Incubator, Medel 2015).

**Inoculum:** *Synechocystis* sp. PCC 6803 were grown from  $-80^\circ\text{C}$  glycerol stock cultures by inoculating 15 mL of BG-11 medium with gentle shaking under 12-h light and dark intervals. The BG-11 contained 1.5 g  $\text{NaNO}_3$ , 40 mg  $\text{K}_2\text{HPO}_4$ , 75 mg  $\text{MgSO}_4$ , 36 mg  $\text{CaCl}_2$ , 1 mg of EDTA, and 6 mg of citric acid and of ferric ammonium citrate per 1 L of distilled water. Fluorescent lamps-controlled chamber provided the continuous aeration at  $30 \pm 2^\circ\text{C}$  and illumination for 2 weeks. Growth was monitored by measuring the optical density at 600 nm ( $\text{OD}_{600}$ ) and the culture reached an  $\text{OD}_{600}$  of 1.2.

**Charging-discharging cycle operation:** Charging-discharging cycles were performed by using a customized electric circuit with the Arduino Software (IDE) for driving relays (Fig. S2). Each relay channel was used to control the on/off states of the external circuit through a resistor.

**Cyclic voltammetry test:** By using AutoLab PGSTAT128N/FRA32 (Metrohm), cyclic voltammetry (CV) was carried out to evaluate the system performance. All CV tests were performed in BG-11 media for 20 cycles from  $-0.7 \text{ V}$  to  $0.6 \text{ V}$  at a scan rate of  $50 \text{ mV/s}$ .

**Bacterial Fixation and SEM Imaging:** The SEM samples were treated with 4% glutaraldehyde solution (Sigma-Aldrich) overnight at  $4^\circ\text{C}$  and rinsed three times with 0.1 M phosphate buffer saline (PBS). The samples were then dehydrated by 5-min serial transfers through 50, 70, 80, 90, 95, and 100% ethanol. The samples were placed in hexamethyldisilizane (HMDS) right after for 10 min and then placed in desiccator to air dry overnight. Fixed samples were examined using a FESEM (Field Emission SEM) (Supra 55 VP, Zeiss).

### CRediT authorship contribution statement

**Lin Liu:** Investigation, Methodology, Data curation, Writing - original draft. **Seokheun Choi:** Conceptualization, Supervision, Project administration, Funding acquisition, Writing - review & editing.

### Acknowledgments

This work is supported by the Office of Naval Research (#N00014-81-1-2422), National Science Foundation (ECCS #1703394), and the SUNY Binghamton Research Foundation (SE-TAE).

## Appendix A. Supplementary data

Supplementary data to this article can be found online at <https://doi.org/10.1016/j.bios.2019.111354>.

## References

Alsaoub, S., Ruff, A., Conzuelo, F., Ventosa, E., Ludwig, R., Shleev, S., Schuhmann, W., 2017. An intrinsic self-charging biosupercapacitor comprised of a high-potential bioanode and a low-potential biocathode. *ChemPlusChem* 82, 576–583.

Bombelli, P., Bradley, R.W., Scott, A.M., Philips, A.J., McCormick, A.J., Cruz, S.M., Anderson, A., Yunus, K., Bendall, D.S., Cameron, P.J., Davies, J.M., Smith, A.G., Howe, C.J., Fisher, A.C., 2011. Quantitative analysis of the factors limiting solar power transduction by *Synechocystis* sp. PCC6803 in biological photovoltaic devices. *Energy Environ. Sci.* 4, 4690–4698.

Bombelli, P., Zarrouati, M., Thorne, R.J., Schneider, K., Rowden, S.J.L., Alik, A., Yunus, K., Cameron, P.J., Fisher, A.C., Wilson, D.I., Howe, C.J., McCormick, A.J., 2012. Surface morphology and surface energy of anode materials influence power outputs in a multi-channel mediatorless bio-photovoltaic system. *Phys. Chem. Chem. Phys.* 14, 12221–12229.

Bombelli, P., Muller, T., Herling, T.W., Howe, C.J., Knowles, T.R.J., 2015. A high power-density, mediator-free, microfluidic biophotovoltaic device for cyanobacterial cells. *Adv. Energy Mater.* 5, 1401299.

Chen, G.Z., 2017. Supercapacitor and supercapattery as emerging electrochemical energy stores. *Int. Mater. Rev.* 62, 173–202.

Cheng, S., Liu, H., Logan, B.E., 2006. Increased performance of single-chamber microbial fuel cells using an improved cathode structure. *Electrochem. Commun.* 8, 489–494.

Choi, S., 2015. Microscale microbial fuel cells: advances and challenges. *Biosens. Bioelectron. Rev. Artic.* 69, 8–25.

Cook-Chennault, K.A., Thambi, N., Sastry, A.M., 2008. “Powering MEMS portable devices – a review of non-regenerative and regenerative power supply systems with special emphasis on piezoelectric energy harvesting systems. *Smart Mater. Struct.* 17 043001.

Deeke, A., Sleutels, T.H.J.A., Hamelers, H.V.M., Buisman, C.J.N., 2012. Capacitive bioanodes enable renewable energy storage in microbial fuel cells. *Environ. Sci. Technol.* 46, 3554–3560.

Deeke, A., Sleutels, T.H.J.A., Heijne, A.T., Hamelers, H.V.M., Buisman, C.J.N., 2013. Influence of the thickness of the capacitive layer on the performance of bioanodes in microbial fuel cells. *J. Power Sources* 243, 611–616.

Deeke, A., Sleutels, T.H.J.A., Donkers, T.F.W., Hamelers, H.V.M., Buisman, C.J.N., Heijne, A.T., 2015. Fluidized capacitive bioanode as a novel reactor concept for the microbial fuel cell. *Environ. Sci. Technol.* 49, 1929–1935.

Dewan, A., Ay, S.U., Nazmul Karim, M., Beyenal, H., 2014. Alternative power sources for remote sensors: a review. *J. Power Sources* 245, 129–143.

Dubal, D.P., Ayyad, O., Ruiz, V., Gomez-Romero, P., 2015. Hybrid energy storage: the merging of battery and supercapacitor chemistries. *Chem. Soc. Rev.* 44, 1777–1790.

Gonzalez-Arribas, E., Aleksejeva, O., Bobrowski, T., Toscano, M.D., Gorton, L., Schuhmann, W., Shleev, S., 2017. Solar biosupercapacitor. *Electrochem. Commun.* 74, 9–13.

Hatzell, M.C., Kim, Y., Logan, B.E., 2013. Powering microbial electrolysis cells by capacitor circuits charged using microbial fuel cell. *J. Power Sources* 229, 198–202.

Houghton, J., Santoro, C., Soavi, F., Servo, A., Ieropoulos, I., Arbizzani, C., Atanassov, P., 2016. Supercapacitive microbial fuel cell: characterization and analysis for improved charge storage/delivery performance. *Bioresour. Technol.* 218, 552–560.

Hu, Y., Zhang, Y., Xu, C., Lin, L., Snyder, R.L., Wang, Z.L., 2011. Self-powered system with wireless data transmission. *Nano Lett.* 11, 2572–2577.

Katuri, K.P., Scott, K., Head, I.M., Picioreanu, C., Curtis, T.P., 2011. Microbial fuel cells meet with external resistance. *Bioresour. Technol.* 102, 2758–2766.

Kim, J., Kim, J.H., Ariga, K., 2017. Redox-active polymers for energy storage nanoarchitectonics. *Joule* 1, 739–768.

Lea-Smith, D.J., Bombelli, P., Vasudevan, R., Howe, C.J., 1857. Photosynthetic, respiratory and extracellular electron transport pathways in cyanobacteria. *Biochim. Biophys. Acta* 247–255, 2016.

Liu, L., Choi, S., 2017. Self-sustainable, high-power-density bio-solar cells for lab-on-a-chip applications. *Lab Chip* 17, 3817–3825.

Liu, X., Wu, W., Gu, Z., 2015. Poly (3,4-ethylenedioxythiophene) promotes direct electron transfer at the interface between *Shewanella* loihica and the anode in a microbial fuel cell. *J. Power Sources* 277, 110–115.

Malik, S., Drott, E., Griselda, P., Lee, J., Lee, C., Lowy, D.A., Gray, S., Tender, L.M., 2009. A self-assembling self-repairing microbial photoelectrochemical solar cell. *Energy Environ. Sci.* 2, 292–298.

Malvankar, N.S., Mester, T., Tuominen, M.T., Lovley, D.R., 2012. Supercapacitors based on c-type cytochromes using conductive nanostructured networks of living bacteria. *ChemPhysChem* 13, 463–468.

Marzocchi, M., Gualandi, I., Calienni, M., Zironi, I., Scavetta, E., Castellani, G., Fraboni, B., 2015. Physical and electrochemical properties of PEDOT:PSS as a tool for controlling cell growth. *ACS Appl. Mater. Interfaces* 7, 17993–18003.

McCormick, A.J., Bombelli, P., Scott, A.M., Philips, A.J., Smith, A.G., Fisher, A.C., Howe, C.J., 2011. Photosynthetic biofilms in pure culture harness solar energy in a mediatorless bio-photovoltaic cell system. *Energy Environ. Sci.* 4, 4699–4709.

McCormick, A.J., Bombelli, P., Bradley, R.W., Thorne, R., Wenzel, T., Howe, C.J., 2015. Biophotovoltaics: oxygenic photosynthetic organisms in the world of bioelectrochemical systems. *Energy Environ. Sci.* 8, 1092–1109.

Pang, S., Gao, Y., Choi, S., 2018a. Flexible and stretchable biobatteries: monolithic integration of membrane-free microbial fuel cells in a single textile layer. *Adv. Energy Mater.* 8, 1702261.

Pang, S., Gao, Y., Choi, S., 2018b. Flexible and stretchable microbial fuel cells with modified conductive and hydrophilic textile. *Biosens. Bioelectron.* 100, 504–511.

Pankratov, D., Falkman, P., Blum, Z., Shleev, S., 2014a. A hybrid electric power device for simultaneous generation and storage of electric energy. *Energy Environ. Sci.* 7, 989–993.

Pankratov, D., Blum, Z., Suyatin, D.B., Popov, V.O., Shleev, S., 2014b. Self-charging electrochemical biocapacitor. *ChemElectroChem* 1, 343–346.

Pankratov, D., Blum, Z., Shleev, S., 2014c. Hybrid electric power biodevices. *ChemElectroChem* 1, 1798–1807.

Pankratova, G., Pankratov, D., Hasan, K., Akerlund, H., Albertsson, P., Leech, D., Shleev, S., Gorton, L., 2017. Supercapacitive Photo-Bioanodes and Biosolar Cells: a novel approach for solar energy harnessing. *Adv. Energy Mater.* 7, 1602285.

Park, H., Ko, S., Park, J., Kim, J.Y., Song, H., 2013. Redox-active charge carriers of conducting polymers as a tuner of conductivity and its potential window. *Sci. Rep.* 3, 2454.

Picioreanu, C., van Loosdrecht, M.C., Katuri, K.P., Scott, K., Head, I.M., 2008. Mathematical model for microbial fuel cells with anodic biofilms and anaerobic digestion. *Water Sci. Technol.* 57, 965–971.

Qian, Z., Kang, S., Rajaram, V., Cassella, C., McGruer, N.E., Rinaldi, M., 2017. Zero power infrared digitizers based on plasmonically-enhanced micromechanical photoswitches. *Nat. Nanotechnol.* 12, 969–973.

Rajaram, V., Qian, Z., Kang, S., Calisgan, S.D., McGruer, N.E., Rinaldi, M., 2018. Zero-power electrically tunable micromechanical photoswitches. *IEEE Sens. J.* 18, 7833–7841.

Ren, S., Xia, X., Yuan, L., Liang, P., Huang, X., 2013. Enhancing charge harvest from microbial fuel cells by controlling the charging and discharging frequency of capacitors. *Bioresour. Technol.* 146, 812–815.

Ren, H., Tian, H., Lee, H., Park, T., Leung, F.C., Ren, T., Chae, J., 2015. Regulating the respiration of microbe: a bio-inspired high performance microbial supercapacitor with graphene based electrodes and its kinetic features. *Nano Energy* 15, 697–708.

Sekar, N., Ramasamy, R.P., 2015. Recent advances in photosynthetic energy conversion. *J. Photochem. Photobiol. C Photochem. Rev.* 22, 19–33.

Selvan, K.V., Ali, M.S.M., 2016. Micro-scale energy harvesting devices: review of methodological performances in the last decade. *Renew. Sustain. Energy Rev.* 54, 1035–1047.

Singh, O.V., Gabani, P., 2011. Extremophiles: radiation resistance microbial reserves and therapeutic implications. *J. Appl. Microbiol.* 110, 851–861.

Soavi, F., Bettini, L.G., Piseri, P., Milani, P., Santoro, C., Atanassov, P., Arbizzani, C., 2016. Miniaturized supercapacitors: key materials and structures towards autonomous and sustainable devices and systems. *J. Power Sources* 326, 717–725.

Uria, N., Berbel, X.M., Sanchez, O., Munoz, F.X., Mas, J., 2011. Transient storage of electrical charge in biofilms of *Shewanella oneidensis* MR-1 growing in a microbial fuel cell. *Environ. Sci. Technol.* 45, 10250–10256.

Villarrubia, C.W.N., Soavi, F., Santoro, C., Arbizzani, C., Serov, A., Rojas-Carbonell, S., Gupta, G., Atanassov, P., 2016. Self-feeding paper based biofuel cell/power hybrid  $\mu$ -supercapacitor integration system. *Biosens. Bioelectron.* 86, 459–465.

Volkov, A.V., Wijeratne, K., Mitraka, E., Ail, U., Zhao, D., Tybrant, K., Andreasen, J.W., Berggren, M., Crispin, X., Zozoulenko, I.V., 2017. Understanding the capacitance of PEDOT:PSS. *Adv. Funct. Mater.* 27, 1700329.

Wang, Z.L., Wu, W., 2012. Nanotechnology-enabled energy harvesting for self-powered micro-nanosystems. *Angew. Chem. Int. Ed.* 51, 2–24.

Wei, X., Lee, H., Choi, S., 2016. Biopower generation in a microfluidic bio-solar panel. *Sensor. Actuator. B Chem.* 228, 151–155.

Wu, F., Rudiger, C., Yuce, M.R., 2017. Real-time performance of a self-powered environmental IoT sensor network system. *Sensors* 17, 282.

Xiao, X., Conghaile, P.O., Leech, D., Ludwig, R., Magner, E., 2017. A symmetric supercapacitor/biofuel cell hybrid device based on enzyme-modified nanoporous gold: an autonomous pulse generator. *Biosens. Bioelectron.* 90, 96–102.

Zanella, A., Bui, N., Castellani, A., Vangelista, L., Zorzi, M., 2014. Internet of Things for smart cities. *IEEE Internet Things J.* 1, 22–32.